

See discussions, stats, and author profiles for this publication at: <https://www.researchgate.net/publication/45535340>

Melting of a β -Hairpin Peptide Using Isotope-Edited 2D IR Spectroscopy and Simulations

ARTICLE *in* THE JOURNAL OF PHYSICAL CHEMISTRY B · SEPTEMBER 2010

Impact Factor: 3.3 · DOI: 10.1021/jp104017h · Source: PubMed

CITATIONS

63

READS

54

8 AUTHORS, INCLUDING:



Adam Smith

University of Akron

34 PUBLICATIONS 801 CITATIONS

[SEE PROFILE](#)



Chunte Sam Peng

Massachusetts Institute of Technology

18 PUBLICATIONS 213 CITATIONS

[SEE PROFILE](#)



Andrei Tokmakoff

University of Chicago

153 PUBLICATIONS 8,012 CITATIONS

[SEE PROFILE](#)



Thomas La Cour Jansen

University of Groningen

78 PUBLICATIONS 1,708 CITATIONS

[SEE PROFILE](#)

Melting of a β -Hairpin Peptide Using Isotope-Edited 2D IR Spectroscopy and Simulations

Adam W. Smith,[†] Joshua Lessing, Ziad Ganim, Chunte Sam Peng, and Andrei Tokmakoff*

Department of Chemistry, Massachusetts Institute of Technology, 77 Massachusetts Avenue, Cambridge, Massachusetts 02139

Santanu Roy, Thomas L. C. Jansen, and Jasper Knoester

Center for Theoretical Physics and Zernike Institute for Advanced Materials, University of Groningen, Nijenborgh 4, 9747 AG Groningen, The Netherlands

Received: May 3, 2010

Isotope-edited two-dimensional infrared spectroscopy has been used to characterize the conformational heterogeneity of the β -hairpin peptide TrpZip2 (TZ2) across its thermal unfolding transition. Four isotopologues were synthesized to probe hydrogen bonding and solvent exposure of the β -turn (K8), the N-terminus (S1), and the midstrand region (T10 and T3T10). Isotope-shifts, 2D lineshapes, and other spectral changes to the amide I 2D IR spectra of labeled TZ2 isotopologues were observed as a function of temperature. Data were interpreted on the basis of structure-based spectroscopic modeling of conformers obtained from extensive molecular dynamics simulations. The K8 spectra reveal two unique turn geometries, the type I' β -turn observed in the NMR structure, and a less populated disordered or bulged loop. The data indicate that structures at low temperature resemble the folded NMR structure with typical cross-strand hydrogen bonds, although with a subpopulation of misformed turns. As the temperature is raised from 25 to 85 °C, the fraction of population with a type I' turn increases, but the termini also fray. Hydrogen bonding contacts in the midstrand region remain at all temperatures although with increasing thermal disorder. Our data show no evidence of an extended chain or random coil state for the TZ2 peptide at any temperature. The methods demonstrated here offer an approach to characterizing conformational variation within the folded or unfolded states of proteins and peptides.

Introduction

Protein conformational dynamics lie at the heart of numerous biophysical processes, including protein folding, substrate binding, molecular recognition, and self-assembly. Historically, such processes were often conceived in terms of rigid protein molecules with minimal conformational degrees of freedom. However, structure formation in such processes involves a complex interplay between the favorable energy of contact formation and conformational entropy. Protein flexibility and conformational heterogeneity are intrinsic to all systems, but this disorder and its role in biophysical processes remains difficult to study and describe experimentally. This stems from a paucity of methods that can explore these questions. Conformational dynamics occur over picosecond and longer time-scales, and atomistic structural resolution in solution is only routinely available from computer simulations. The most detailed experimental observations have emerged from magnetic resonance spin relaxation rate measurements that characterize inherently disordered proteins,¹ residue-level protein folding,² transient protein–protein complexes,^{3,4} and microsecond structural fluctuations.^{5–8}

Two-dimensional infrared spectroscopy (2D IR) is an emerging method that is being used to directly measure structure and conformational dynamics in proteins and peptides.^{9–14} Analogous to multidimensional NMR, 2D IR observes structure-sensitive vibrational couplings through cross peaks in a 2D

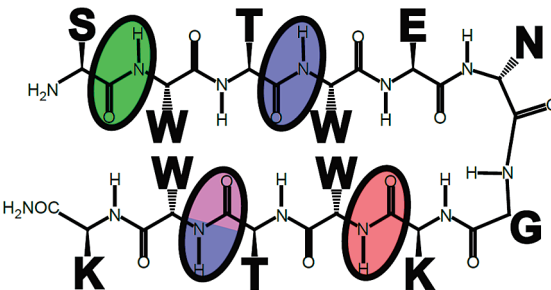


Figure 1. Structure of TZ2 highlighting the S1 (green), TT (blue), T10 (purple), and K8 (pink).

spectrum.¹⁵ In addition, 2D lineshapes provide information on molecular flexibility and solvent exposure through their peak frequency and ellipticity. Time-dependent changes to cross peaks and lineshapes reveal chemical exchange processes and fluctuations. Since the measurement time scale for vibrational spectroscopy is in the picosecond range, such studies provide an avenue to characterize conformational variation and ultrafast fluctuations. The technique has been used to measure protein structure and dynamics with particular focus on the amide I vibrations, which are sensitive to secondary structure and local hydrogen bonding geometry of the peptide groups.^{9–12,16–20}

This paper describes our investigation of the structure of a β -hairpin peptide using isotope-edited 2D IR to site-specifically investigate the conformation of its backbone as a function of temperature. In this mode, the isotope-shifted amide I band can

* Corresponding author. Telephone: 617-253-4503. Fax: 617-253-7030. E-mail: tokmakof@mit.edu.

[†] Present address: Department of Chemistry, University of California, Berkeley, 424 Stanley Hall, Berkeley, CA 94720.

Adam W. Smith earned his Bachelor's degree from the University of Utah in Chemical Physics. His Ph.D. work was done with Andrei Tokmakoff at MIT studying peptide dynamics with 2D IR spectroscopy and site-specific isotope labeling. He is currently a HHMI postdoctoral associate at U.C. Berkeley with Jay T. Groves where he studies protein organization and dynamics in the plasma membrane of living cells.

Joshua Lessing received his Sc.B. in Chemistry from Brown University in 2004. Upon graduation he was a postbaccalaureate student in the Rose-Petruck lab at Brown University studying ultrafast XAFS spectroscopy, liquid structure, and molecular dynamics. In 2005 he began a Ph.D. program under the direction of Andrei Tokmakoff working to elucidate the fundamental design principles governing the elasticity and durability of elastin-based biopolymers.

Ziad Ganim obtained his B.S. in Chemistry from the University of California at Berkeley in 2003, and will obtain his Ph.D. from MIT in 2010. His research interests include using ultrafast infrared spectroscopy and single molecule techniques for studying protein–protein interactions.

Chunmei Peng grew up in Taiwan and came to the United States in 2004 to pursue his college degree from the University of California at Berkeley. After graduating with a B.S. in Chemistry in 2008, he started graduate school at M.I.T. and is now working in the Tokmakoff group. He is interested in protein folding and self-assembly problems studied by 2D IR spectroscopy.

Andrei Tokmakoff received his Ph.D. from Stanford University in 1995 under the direction of Michael Fayer. Following postdoctoral positions with Alfred Laubereau (Technical University Munich) and Graham Fleming (UC Berkeley), he joined the faculty at MIT in 1998.

Santanu Roy is currently a Ph.D. student at the Center for Theoretical Physics and the Zernike Institute for Advanced Materials, University of Groningen. He is working under the supervision of Dr. Thomas la Cour Jansen and Prof. Jasper Knoester. He is interested in the theoretical investigation of fast protein folding/unfolding dynamics with MD simulation and 2DIR spectroscopy. He received his M.Sc. degree in Physics from University of Pune, India in 2006 and B.Sc. degree in Physics (Hons) from University of Calcutta in 2004.

Thomas la Cour Jansen is a tenure-track assistant professor in Computational Spectroscopy at the University of Groningen. He received his Ph.D. from the University of Groningen in 2002 (cum laude) working with Prof. Jaap G. Snijders and Prof. Koos Duppen. He then did postdoctoral work with Prof. Shaul Mukamel at the University of Rochester and University of California at Irvine. His research interests are developing methods for modeling multidimensional spectroscopy and applying these to solve questions about structure and dynamics in condensed-phase systems.

Jasper Knoester received his Ph.D. from the University of Utrecht in 1987, followed by postdoctoral work in the group of Shaul Mukamel at the University of Rochester. In 1989 he started working in Groningen, first as a Huygens fellow in the group of Douwe A. Wiersma, and from 1993 onwards as professor of theoretical condensed matter physics. His research focuses on the optical properties and excited state dynamics of supramolecular and nanostructured materials. Currently, he is Dean of the Faculty of Mathematics and Natural Sciences.

be used to infer local structure and dynamics through variations in its vibrational frequency or couplings to other vibrations. Our approach combines 2D IR spectroscopy on a series of peptide isotopologues with spectroscopic modeling of the peptide's conformers. This pair of tools is used to develop a picture of conformational heterogeneity across the thermal unfolding transition.

The system that is studied is a 12-residue hairpin peptide trpzip2 (TZ2) designed by Cochran et al.²¹ It has received significant attention in the literature, with multiple experimental studies and numerous theoretical treatments.^{17,22–27} Within the last several years, TZ2 has become a benchmark system which is now used in the development of new simulation techniques.^{22,26,28–30} The trpzip peptides were engineered with four tryptophan residues arranged with two side chains on each of the opposing β -strands that lead to a remarkably stable system through the favorable perpendicular stacking of the indole rings.²¹ Our interest in this system is motivated by unsolved questions

regarding the folding of these peptides. Single-domain peptides like β -hairpins display conformational dynamics that mirror the folding of larger globular proteins.^{31,32} Discussion of hairpin folding mechanisms are often guided by two simple pictures: (1) the kinetic zipper model, in which nucleation of the β -turn is followed by “zipping” of cross-strand backbone contacts,^{33–35} and (2) hydrophobic collapse, in which initial clustering by a core of hydrophobic side chains precedes formation of native backbone contacts.^{36,37} Extensive fluorescence^{38–40} and IR absorption^{41–43} measurements have monitored the kinetics of hairpin unfolding on 1–10 μ s time scales but have not reached agreement on which model best describes the folding.^{41,43,44} Often, folding of this peptide is described within the framework of a two-state folding model, although its validity and the nature of the two states is unclear.⁵

Molecular dynamics (MD) simulations of TZ2 folding have provided intricate details that enrich and challenge these two models, such as partial hydrophobic collapse, fraying of the terminal residues, ordering of backbone hydrogen bonds, salt bridging, and rearrangements of the hydrophobic core.^{30,45,46} To date, however, the complex set of possible folding pathways observed by simulations have not led to a consensus view of the folding mechanism. Experimental evidence has substantiated this complexity and supports a rough free energy landscape in which there are a number of populated minima.³⁰ To date, the structural details of this heterogeneity have not been experimentally observed, particularly in the peptide backbone. The key information missing from these studies is specific details of hydrogen bond and side chain contact formation at a level of detail that can distinguish conformers.

To obtain residue-level structural insight in the thermal denaturation of TZ2, we use amide I 2D IR in combination with ¹³C and ¹⁸O isotope-labeling methods.^{11,18–20,47–52} Inserting these labels into the peptide amide group red shifts the amide I vibrational frequency away from the main band and provides a spectroscopic probe of the labeled site. Four isotopologues are used to probe cross-strand contacts and isolate peptide units in the turn, termini, and central region of the folded structure (see Figure 1).

In the first isotopologue, S1, an ¹⁸O isotope is introduced into the N-terminal serine to probe the stability and fraying of the terminal peptide groups. In the second, T10, an ¹⁸O label is placed on the T10 site to monitor the midstrand contacts. The third, TT, also monitors midstrand contacts using ¹³C isotope-labels at threonines T3 and T10 of the peptide. The two labeled amides of TT are hydrogen bound across the β -strands in the folded structure, and vibrational coupling between these sites provides sensitivity to the interstrand contacts in this region.⁵³ Finally, the isotopologue K8 has a ¹³C label incorporated into the lysine-8 residue to probe the thermal disordering of the β -turn.

The interpretation of 2D IR spectra uses a structure-based spectroscopic model that draws on molecular dynamics simulations of the TZ2 peptide in water. Our spectral simulations make use of the extensive set of TZ2 conformers obtained from the molecular dynamics simulations of Swope and co-workers,^{30,46} and accompanying Markov state analysis of Chodera et al.²⁹ Experimental amide I frequency shifts and 2D lineshapes are assigned and interpreted on the basis of calculated 2D spectra for these Markov states. Spectra are calculated using the local amide I Hamiltonian that describes the amide I frequency shifts of the peptide groups and vibrational couplings between these groups.^{54–57} The amide I site frequencies are mapped onto the local molecular electric field.^{55,56,58,59} This describes the red-

shifting of the amide I frequency upon hydrogen bonding to the peptide unit.

The disorder and local fluctuations of each conformer is reflected in the 2D line shape of the labeled site.^{17,60} The diagonal line width of the 2D IR peak is sensitive to the degree of conformational disorder, whereas the antidiagonal width reflects the fluctuations and time scale of interchange. Therefore the ellipticity of the line shape is inversely related to the time scale over which the vibration samples the possible configurations. A large value of the ellipticity indicates significant disorder in the corresponding local structure. Fast fluctuations in structure and hydrogen bonded solvent lead to round peaks.⁶¹

This study establishes a detailed picture of the conformational changes upon temperature-induced unfolding of TZ2. The isotopologues provide evidence that the termini disorder as the temperature is raised, and the central region retains cross-strand contacts. Further we find explicit evidence for distinct conformers of the turn, and that the population of the expected type I' turn increases with temperature. Taken together, these observations reveal a temperature varying heterogeneous ensemble, whose conformers all experience thermally induced fraying, but do not unfold into a random coil structure. In addition to this agreement with previous results, the work shown here gives a level of detail unattainable with other methods. Isotope-editing provides structural detail at the level of individual amide groups with higher spectral resolution than FTIR spectroscopy, while resolving picosecond dynamics that report on peptide flexibility and solvent exposure.

Material and Methods

Peptide Samples. For experimental studies, the unlabeled peptide, UL, was prepared using Fmoc-based solid phase peptide synthesis on a PS3 peptide synthesizer (Protein Technologies Inc.). Each TZ2 isotopologue was prepared as a C-terminal amide, which is consistent with previous experimental work. The solid support was a Rink Amide MBHA resin (01-64-0037, Novabiochem), and Fmoc-protected amino acids were obtained from PTI Instruments in prepackaged cartridges at four molar excess HBTU activator and amino acid. The primary reaction solvent was DMF (EM-DX1732; EMD Chemicals; 99.9% purity). Removal of the Fmoc groups at each step was done with 20% piperidine in DMF (PTI Instruments), and the coupling reaction was carried out in 0.4 M *N*-methylmorpholine/DMF activator solution (PTI Instruments). A cleavage cocktail of 95% TFA and 5% TIPS was used to remove the peptide from the resin and the acid-labile protecting groups from the side chains. Purification was performed with a C18 HPLC column and two-phase buffer gradient: (buffer A) 0.1% TFA in H₂O and (buffer B) 80% acetonitrile, 0.085% TFA in H₂O. The mass spectrum of the final product is provided in the Supporting Information.

The midstrand isotope-labeled compound, TT, was prepared with a ¹³C in the C' carbon (identified as *) of the Thr3 and Thr10 residues (SWT*WENGKWT*WK), which shifts the site energy of the Thr3-Trp4 and Thr10-Trp11 amide groups. TT was synthesized and purified by Anaspec Inc. (San Jose, CA) using L-threonine-1-¹³C (Icon Isotopes, Summit, NJ) as reported previously.⁶² The mass spectrum is provided in the Supporting Information.

The turn-region isotope-labeled compound, K8, was prepared with a ¹³C atom in the C' position of the Lys8 residue (SWTWENGK*WTWK). Peptide synthesis was performed identically to that of UL outlined above. Isotope-labeled lysine (*L*-lysine- α -N-FMOC, ϵ -*N*-*t*-BOC) was purchased from Cam-

bridge Isotope Laboratories (CLM-6194, 1-¹³C, 99%) and used without any modification in the synthesis and purification procedures. The mass spectrum of synthesized K8 is provided in the Supporting Information.

The N-terminal label, S1, was prepared with an ¹⁸O label in the carbonyl oxygen (identified as †) of the S1 residue (S†WTWENGKWTWK). Labeled serine was synthesized directly from Fmoc-serine-OH (Novabiochem) using acid catalyzed hydrolysis. Anhydrous HCl gas was bubbled through Fmoc-Ser-OH in H₂¹⁸O:acetonitrile (approximately 1:4 by volume), and then heated at 80 °C for four weeks. MALDI mass spectrometry of the amino acid was used to verify that the substitution was successful, with an approximately 75% isotopic enrichment of the carboxyl oxygen atoms. For use in peptide synthesis, the serine hydroxyl group was protected by a silylation reaction using *N*-methyl-*N*-(*tert*-butyldimethylsilyl)-trifluoroacetamide (MTBSTFA) in the procedure of Madson et al.⁶³ Specifically, 139 mg of ¹⁸O labeled serine was dissolved in 15 mL of DMF and 3 mL of MTBSTFA, where it silylates both the side chain hydroxyl group and the carboxylic acid. The reaction solution was lyophilized and the remaining peptide was then suspended in hexane (20 mL). Ethanol (1.1 mol excess relative to Ser) was added to selectively desilylate the carboxylic acid. The resulting amino acid was used in an Fmoc-SPPS synthesis identical to that of UL. MALDI-TOF mass spectrometry of the labeled TZ2-S1 verified the mass of the isotope-labeled peptide indicating that the isotope-labeled serine was incorporated into the peptide (Supporting Information).

The midstrand label, T10, was prepared with an ¹⁸O label in the carbonyl oxygen using the same method as described above for the N-terminal ¹⁸O S1 label.

For infrared studies, residual TFA was removed from each peptide by lyophilizing against 20 mM DCl in D₂O repeated at least three times. This also served to exchange the labile protons for deuterons. For FTIR spectra, each peptide was dissolved in pure D₂O, and the pH was adjusted to 2.5 by adding 0.5–1.5 μ L of 25 mM DCl. The low pH was chosen to avoid aggregation while measurements are being taken at high temperatures. Final peptide concentrations were between 10 and 12 mg/mL. The 2D IR spectra of UL, S1, and K8 were taken in a phosphate-buffered pH 7.0 solution at similar concentrations.

Spectroscopic Methods. Temperature dependent infrared absorption spectra of each peptide isotopologue were collected from 5 to 95 °C in 5 °C increments. The sample cell used in these measurements consists of ~25 μ L of the peptide solution sandwiched between two 1 mm thick CaF₂ windows that are separated by a 50 μ m Teflon spacer. For temperature control, the cell was mounted in a brass housing whose temperature was regulated with water from a recirculating chiller. Spectra were acquired on a Nicolet 380 FTIR spectrometer at 1.0 cm⁻¹ spectral resolution by averaging 64 one-second scans.

2D IR spectra were collected as described in previous publications,¹⁵ with τ_2 = 100 fs and the polarization geometry all parallel (ZZZZ) unless otherwise noted. The evolution time, τ_1 , was scanned to 1.5 ps for the nonrephasing spectrum and 2.0 ps for the rephasing spectrum at 4 fs time steps, and a rectangular window function was used for the Fourier transform.

Simulation and Modeling. To simulate 2D IR spectra, five kinetically metastable macrostates were chosen from the decomposition made by Chodera et al.²⁹ Their work distilled the 3.23 μ s of trpzip2 simulation data by Pitera et al.⁴⁶ into 40 Markov states that displayed patterns in backbone hydrogen bonds and side chain packing. Each macrostate, which was

comprised of 30 structurally related microstates with atomistic coordinates, was chosen to represent a different structural model of TZ2.

All molecular dynamics simulations were performed with GROMACS 3.3.1.^{64,65} The simulations of Pitera et al.⁴⁶ considered the unblocked peptide, which was fully protonated here (+3 charge) with chloride counterions. Each of the atomistic structures comprising the macrostate was subjected to ~5000 steps of a steepest descent energy minimization to conform to the OPLS/AA force field^{66–72} using the particle mesh Ewald method to treat long-range electrostatics.⁷³ The peptides were solvated in a box of rigid SPC/E water⁷⁴ that extended 1.5 nm from the solute, and the water was allowed to equilibrate for 10 ps in the NPT ensemble (300 K, 1 atm) while the peptide was fixed.^{75–78} The simulation was continued with no constraints, except on the bond lengths, for 1 ns of equilibration and 100 ps of data acquisition. Structures were saved every 20 fs to yield 5000 frame trajectories.

For each frame, a Hamiltonian was constructed using the ab initio based models given in refs 57 and 58

$$H_S = \sum_i \left(\omega_i B_i^\dagger B_i - \frac{1}{2} \Delta_i B_i^\dagger B_i^\dagger B_i B_i \right) + \sum_{i,j} J_{ij} B_i^\dagger B_j$$

where B_i^\dagger and B_i are bosonic creation and annihilation operators for a vibration at site i . The frequency of each site and the coupling between sites are given by ω_i and J_{ij} respectively. The anharmonicity, Δ_i , lowers the energy for double excitation of site i , and was fixed at 16 cm⁻¹. The frequencies and coupling values were calculated as previously described.^{57,58} The transition dipoles for each site had a unit magnitude and were oriented 20° off the CO bond vector in the CN direction. Where applicable, the sites were isotope-labeled by shifting their frequency 41 cm⁻¹ to the red.

The 2DIR spectra were calculated using the numerical integration of the Schrödinger equation (NISE) scheme.^{79,80} In this procedure the time-evolution matrices needed in the nonlinear response functions that govern the 2DIR spectra are calculated by solving the time-dependent Schrödinger equation. This is done numerically by dividing time into small intervals during which the Hamiltonian can safely be assumed to be constant. The time-evolution matrix for the time-independent Schrödinger equation can then be found for each interval and the time-evolution matrices for longer time periods are found by multiplying the matrices for the small intervals in a time ordered fashion. The resulting spectra were summed over each structure in the macrostate to produce spectra that reflected the disordered ensembles.

Results

Amide I' FTIR Spectroscopy. FTIR spectra of the TZ2 isotopologues at 25 °C are shown in Figure 2. The peak maximum of the UL amide I' band is 1636 cm⁻¹, and there is a prominent shoulder at 1674 cm⁻¹. On the basis of the NMR structure, these bands have previously been assigned to ν_\perp and ν_\parallel excitonic transitions, delocalized vibrations of the amide backbone in which cross-strand peptide bonds oscillate in-phase or out-of-phase with one another.^{53,62} Twisting of the β -strands leads to two nearly degenerate ν_\perp vibrations located at the turn and midstrand regions of the peptide, while the ν_\parallel vibration is largely localized at the turn. Because the spectra shown are taken at pH 2.5, the glutamic acid side chain carbonyl stretch contributes at 1710 cm⁻¹.⁸¹

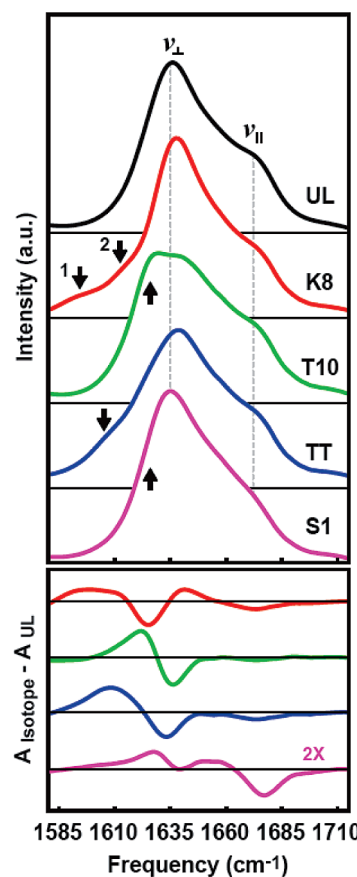


Figure 2. Equilibrium FTIR spectra are shown for each TZ2 isotopologue at 25 °C and pH 2.5. Each spectrum is baseline corrected with a linear subtraction, and area normalized for comparison. Difference data (bottom) are obtained by subtracting the unlabeled spectrum (TZ2-UL) from each of the spectra. The S1 difference spectra is presented at 2× magnification for clarity. Arrows have been drawn to emphasize the isotope labeled peaks.

Changes to the IR spectrum upon isotope substitution are also plotted in Figure 2 for K8, T10, TT and S1. Isotope-labeling leads to small shifts in intensity and frequency of the ν_\perp and ν_\parallel bands, and an increase of amplitude to the red of the bands from the isotope-labeled peptide carbonyl. As seen in difference spectra relative to UL, K8 has a broad (~35 cm⁻¹) increase in intensity from $\nu_{K8} = 1585–1615$ cm⁻¹, indicating significant structural heterogeneity at this site. The ν_\perp band of K8 narrows and shifts slightly to the blue (1638 cm⁻¹), suggesting that isotopic substitution significantly rearranges the underlying ν_\perp eigenstate composition.

In addition to a drop of intensity in the ν_\perp band, the T10 spectrum shows a pronounced shoulder at 1627 cm⁻¹ due to the labeled peptide group. This is a relatively high frequency, indicative of a single moderately strong hydrogen bond to the oxygen as expected from the NMR structure. Upon labeling both threonines (TT), spectral loss is observed at 1640 and 1675 cm⁻¹, and a broad absorbance gain is observed at $\nu_{TT} = 1610$ cm⁻¹. The additional red shift of ν_{TT} relative to ν_{T10} reflects the strength of coupling between the cross-strand labeled oscillators of the ν_{TT} band. Labeling both of the threonine residues red-shifts the midstrand ν_\perp vibration and also perturbs the high frequency, ν_\parallel , band.⁶² A similar but narrower band was observed at 1608 cm⁻¹ for the TZ2 mutant TZ2-T3A*T10A*.²⁵

The FTIR spectrum of S1 is qualitatively similar to the UL spectrum. The peak absorption frequency is red-shifted by 2 cm⁻¹ relative to UL, and the difference spectrum reveals a slight

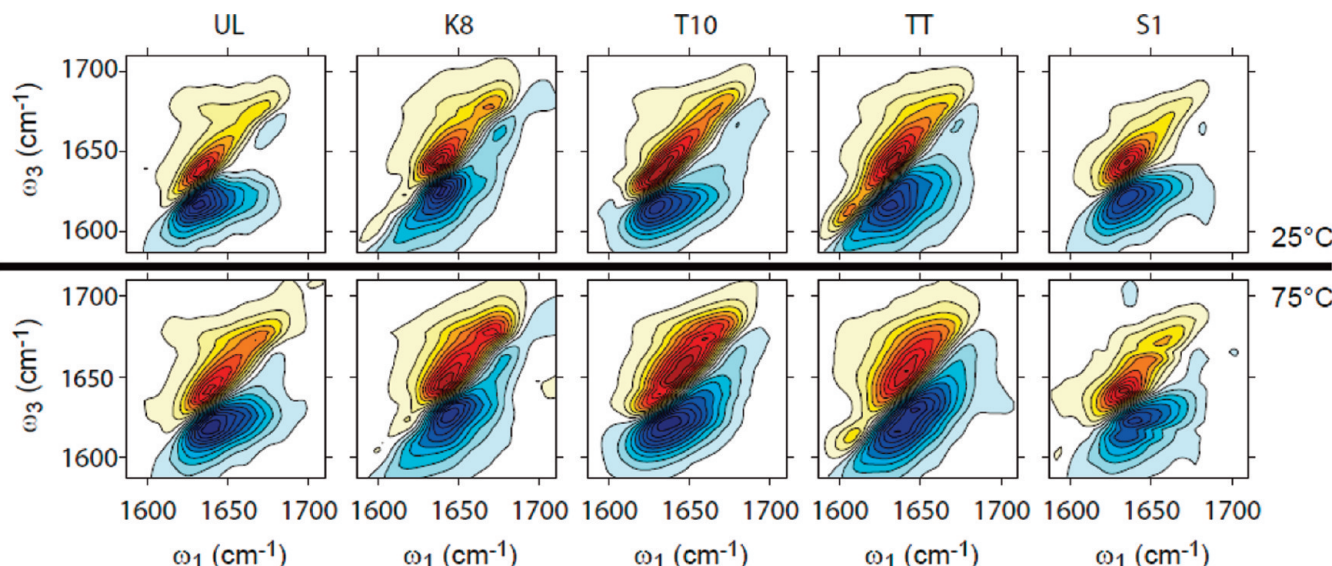


Figure 3. 2D IR Spectra of TZ2 isotopologues at 25 °C (top) and 75 °C (bottom).

intensity increase between 1590 and 1625 cm⁻¹. A distinct ν_{S1} band is unresolved in the FTIR spectrum, which indicates that the 39 cm⁻¹ frequency shift from the ¹⁸O label moves intensity from the blue side of the amide band to the red side, where it remains hidden underneath the ν_{\perp} band. There is also loss from 1670 to 1685 cm⁻¹ and from 1637 to 1650 cm⁻¹ in the difference spectrum.

Amide I' 2D IR Spectroscopy. 2D IR spectra of the TZ2 isotopologues at 25 °C are shown on the top row of Figure 3. The spectra show on and off-diagonal features in the amide I main band between 1630–1690 cm⁻¹, as well as red-shifted features along the diagonal for the isotope-labeled species. Positive features arise from fundamental ($\nu = 0–1$) vibrational transitions, whereas negative features arise from $\nu = 1–2$ transitions. As described previously,²⁴ the UL spectrum shows the Z-shaped contour profiles of the excitonic amide I' bands expected for antiparallel contacts between two strands. The ν_{\parallel} band is resolved as a separate peak rather than a shoulder as in FTIR, and the peak splitting between ν_{\perp} and ν_{\parallel} peaks is 37 cm⁻¹ in the ω_1 dimension. Coupling between ν_{\perp} and ν_{\parallel} vibrations is observed in the off-diagonal region as ridges that extend along $\omega_3 = 1636$ and 1674 cm⁻¹.

For K8, the most striking feature in the 2D IR spectrum is the observation that the ν_{K8} band is composed of two distinct diagonal peaks: one at 1593 cm⁻¹ (ν_{K8-1}) and the other at 1611 cm⁻¹ (ν_{K8-2}), with no detectable cross peak between them. (See also Figure 6.) Also, the diagonal line width of ν_{K8-1} ($\sigma = 6.9$ cm⁻¹) is broader than ν_{K8-2} ($\sigma = 4.5$ cm⁻¹). Strong coupling of the ν_{K8-2} to the ν_{\perp} band is observed as a ridge extending to $\omega_1 = 1612$ cm⁻¹ and $\omega_3 = 1650$ cm⁻¹ (Figure 6). The presence of two shifted peaks for a single K8 isotope-label is an indication of two structurally distinct subensembles. The 18 cm⁻¹ peak splitting between these features indicates that the conformers differ considerably in hydrogen bonding configuration to the K8 peptide oxygen. The relatively high frequency of ν_{K8-2} indicates a single hydrogen bond to oxygen. The most reasonable explanation for this observation is that the ν_{K8-2} peak originates in a properly folded type I' turn in which the labeled oxygen has a single cross-strand hydrogen bond. The ν_{K8-1} peak frequency is characteristic of a peptide group with two or more hydrogen bonds and a higher degree of configurational freedom. This suggests a solvent exposed carbonyl that might be present in a disordered or bulged turn.

For T10, the main excitonic band retains the Z-shaped contours of UL, but an additional sharp peak from the labeled site is observed at $\omega_1 = \omega_3 = 1630$ cm⁻¹. Like ν_{K8-2} this high frequency is suggestive of a single hydrogen bond to oxygen as seen in the NMR structure. In the 2D IR spectrum of the double labeled species, TT, the ν_{TT} band is well-resolved at 1602 cm⁻¹, and the splitting between ν_{\perp} and ν_{TT} in the ω_1 dimension is 28 cm⁻¹. The additional red-shift relative to T10 arises from strong coupling between the Thr3 and Thr10 amides forming a midstrand ν_{\perp} -like mode.⁶² Changes to the 2D IR ν_{\perp} band relative to the other isotopologues are dramatic, including loss of off-diagonal structure and a diagonal line width increase of approximately 21 cm⁻¹. This line width change suggests that the eigenstate distribution of TZ2-TT is much more heterogeneous than in the other peptides.

The 2D IR spectrum of S1 does not show a peak corresponding to the ¹⁸O label in the serine group; however, there are changes relative to UL along the diagonal. The ν_{\parallel} band of the S1 2D IR spectrum, which has a resolvable peak at 1674 cm⁻¹ in the UL spectrum, now appears as a diagonal ridge to the blue of the ν_{\perp} band. In addition there is a 2 cm⁻¹ red-shift to 1634 cm⁻¹ and line-narrowing of the ν_{\perp} peak. These observations indicate that the frequency of the UL S1 site energy is relatively high (~1675 cm⁻¹) and that labeling moves the oscillator into resonance with the ν_{\perp} exciton band. This would also explain the lack of both a resolvable peak and interstrand coupling observed between labeled residues in the TZ2 mutant TZ2-S1A*,T10A*.²⁵

Temperature-Dependent Spectra. Temperature-dependent amide I' FTIR spectra of each isotope-labeled hairpin are shown in Figure 4. Each spectrum shows similar trends with temperature, including the loss of amplitude in the ν_{\perp} region and rise of amplitude in the 1660 cm⁻¹ region commonly attributed to disordered chains. To characterize the overall melting behavior, singular value decomposition (SVD) of the entire amide I' band is carried out for each data set. For each isotopologue, the data is well described with the first two spectral components. Spectral changes with temperature are characterized by the second SVD component, and are shown as melting curves in Figure 5. The melting curves are nearly identical and each show slight curvature without a distinct cooperative unfolding transition.

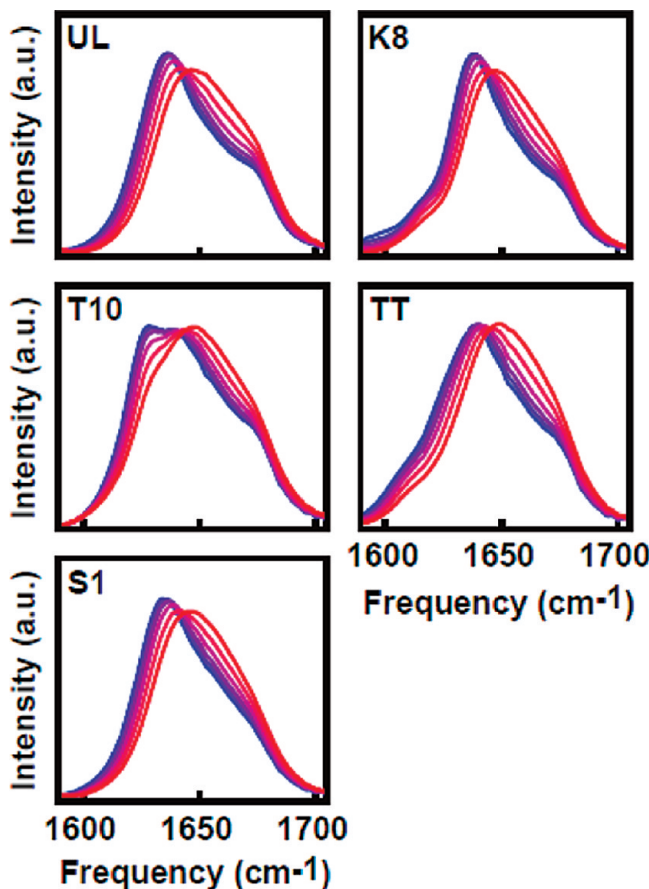


Figure 4. Temperature-dependent FTIR spectra of each TZ2 isotopologue taken from 10 to 85 °C in 15 °C increments (pH 2.5). Line color shows progression from cold (blue) to hot (red).

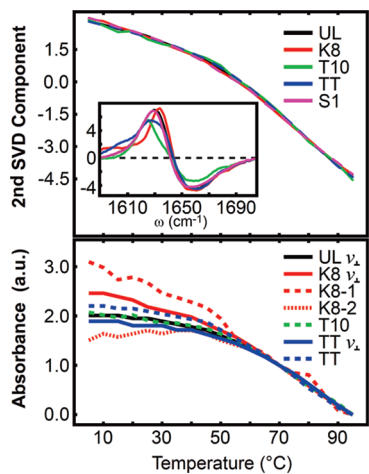


Figure 5. (Top) Second component amplitudes from SVD analysis of the temperature-dependent FTIR spectra. The inset shows the second component spectra. (Bottom) FTIR peak absorbance versus temperature. The ^{12}C peak intensities are obtained from the absorbance within 5 cm^{-1} of the amide I peak maximum. The integration regions for other traces are $\nu_{\text{K8}-1}$, 1588–1598 cm^{-1} ; $\nu_{\text{K8}-2}$, 1612–1619 cm^{-1} ; ν_{TT} , 1603–1611 cm^{-1} . Traces are scaled to overlap between 70 and 95 °C.

This data is consistent with previous IR, fluorescence, and UV-CD measurements^{17,23,24,82} and is identical to the earlier UL data at pH 7.⁶²

In addition to SVD characterization, it is also useful to observe specific spectral regions within the band. The relative

intensities of the isotope-shifted peaks of K8, T10 and TT are compared with the ν_{\perp} peak of UL in Figure 5. Intensities are obtained by averaging the absorbance around the peak positions ($\nu = \pm\sim 5 \text{ cm}^{-1}$), and are compared by overlaying the curves between 70–95 °C. This demonstrates that the melting behavior follows the same trends for all spectroscopic features between 55 and 95 °C. The melting curves for ν_{\perp} peak intensities of all isotopologues have profiles matching the second SVD component melting curves within 10%. Similarly, the intensity of the T10 and TT labels both track the SVD melting curves, suggesting that these curves report on the interstrand contacts in the central region of the peptide. For K8, the $\nu_{\text{K8}-1}$ region changes quasi-linearly with increasing temperature. In contrast, the $\nu_{\text{K8}-2}$ region is largely unchanged for temperatures <40 °C. This melting behavior suggests that the $\nu_{\text{K8}-2}$ peak reports on peptides with a natively structured turn, while the $\nu_{\text{K8}-1}$ peak reports on non-native turn configurations that show a melting curve similar to that expected for a less-stable or disordered peptide. The high apparent melting temperature of the $\nu_{\text{K8}-2}$ peak suggests that the natively structured turn region is in fact more stable than the rest of the peptide and could account for the residual backbone structure previously reported over similar temperatures.

Temperature-dependent changes to the 2D IR spectra of each isotopologue can be seen by comparing the 25 and 75 °C spectra shown in Figure 3. Along the diagonal axis ($\omega_1 = \omega_3$), spectral shifts track those observed in the FTIR data, and spectral features broaden along the antidiagonal axis with increasing temperature. In our analysis, we concentrate on the center frequency, amplitude, and 2D lineshapes of the isotope-labeled features. The line shape can be characterized by their widths parallel and perpendicular to the diagonal axis. The diagonal line width (σ) reflects inhomogeneous broadening that originates in static structural disorder on the time scale of the experiment (~2 ps). Antidiagonal widths (Γ) report on rapid frequency shifts that originate in subpicosecond peptide-solvent interactions and structural fluctuations. The relative magnitudes of these linewidths, or ellipticity $E = (\sigma^2 - \Gamma^2)/(\sigma^2 + \Gamma^2)$,^{61,83} measured as a function of temperature can be used to interpret changes from static disorder to dynamic disorder due to increasing structural flexibility and solvent exposure.⁶¹

Spectral changes to the UL 2D IR data are similar to those reported earlier at pH 7, which were interpreted as fraying of the termini and an intact turn at all temperatures. The antidiagonal line width grows with temperature for both of the β -sheet modes in the 2D IR spectrum (data not shown). The full width at half-maximum (FWHM) of the ν_{\parallel} band is only ~2.0 cm^{-1} larger than that of the ν_{\perp} band at 15 °C, but the slope of the line width increase versus temperature of ν_{\parallel} is twice that of the ν_{\perp} band.

Thermally induced spectral changes to the ν_{K8} peaks can be seen more clearly in Figure 5. As the temperature of the system increases, the spectrum responds both to structural rearrangements and shifting populations between native and misfolded ensembles. The center frequency of the $\nu_{\text{K8}-1}$ and $\nu_{\text{K8}-2}$ bands does not change with temperature, but the amplitudes of both peaks decrease. In addition, the $\nu_{\text{K8}-1}$ intensity decreases with respect to the $\nu_{\text{K8}-2}$ peak, indicating that the native turn is more stable than the disordered turn. Linewidth changes to the TZ2-K8 spectra are consistent with those of the unlabeled hairpin (Figure 7). The slope of the line fit to the FWHM of the ^{12}C ν_{\perp} band ($0.058 \pm 0.012 \text{ cm}^{-1}/\text{°C}$) is twice as large as the corresponding slope of TZ2-UL ($0.020 \pm 0.006 \text{ cm}^{-1}/\text{°C}$). For the $\nu_{\text{K8}-1}$ and $\nu_{\text{K8}-2}$ peaks, the FWHM measurement is noisier

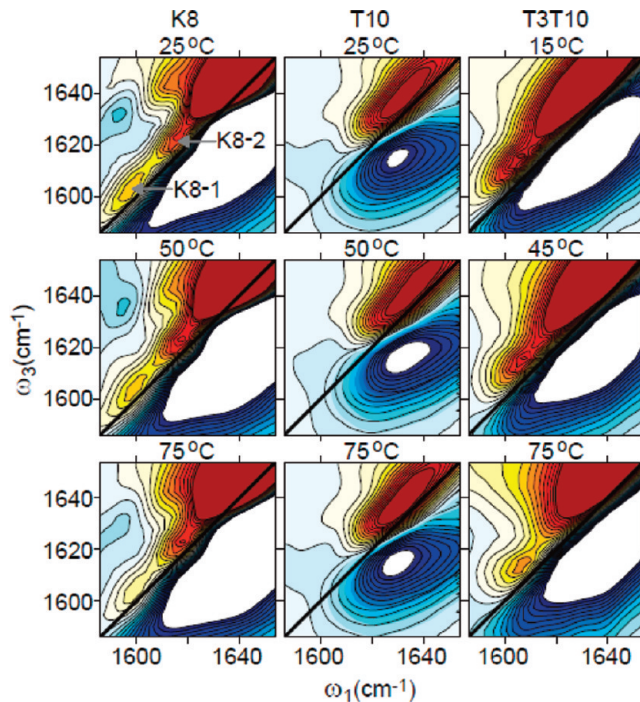


Figure 6. Temperature-dependent 2D-IR spectra of isotope-shifted peaks in K8, T10, and TT. Contour lines are plotted as a percentage of the amide I maximum at the respective temperature. Twenty seven evenly spaced contours are drawn from -18 to $+18\%$ (K8), -80 to $+80\%$ (T10), and -35 to $+35\%$ (TT).

due to lower signal strength. However, the line width of the high frequency peak, ν_{K8-2} , does not display a significant slope with temperature, indicating that the homogeneous broadening does not increase significantly with temperature. The limited resolution of the ν_{K8} peaks prevents a quantitative description of the diagonal line width. However, in the spectra shown in Figure 6 there does not seem to be any clear sign of diagonal peak broadening with temperature.

Together, these observations support the idea that two bands are reporting on subensembles of peptides for which the relative population shifts with temperature, but the line width properties remain relatively constant. The presence of two isotope-shifted peaks in the turn may reflect two distinct conformational states of the peptide; however, from the K8 measurement alone one cannot rule out additional states that have the same type of solvent exposure in the turn. Of course, conformational dynamics will be present that interconvert these turn structures. Not surprisingly, if a two state analysis is applied to this exchange of conformers (K8-1 to K8-2), one finds that the temperature-dependence does not follow van't Hoff behavior (Figure 7). However, if one restricts the analysis to the high temperature range between 45 and 75°C for which most spectral features shift in concert, we find $\Delta H_{1-2} = 20.2 \pm 2.8 \text{ kJ/mol}$.

Thermally induced spectral changes to the ν_{TT} peak are emphasized in Figure 6. Similar to the ν_{K8} peaks, the maximum of the positive diagonal ν_{TT} peak does not shift appreciably with temperature. Instead, the $\nu_{TT} - \nu_{\perp}$ peak splitting increases from 26 cm^{-1} at 15°C to 34 cm^{-1} at 85°C , which results from the blue-shift of the ν_{\perp} peak. The relative intensity of the isotope-shifted peak also drops, going from 40% of the band maximum at 15°C to 20% at 85°C . This decrease in intensity is partially ascribed to a loss of coupling between isotope-labeled amide groups and the ^{12}C amides. The shape of the ν_{TT} peak also changes drastically with temperature, going from a diagonally

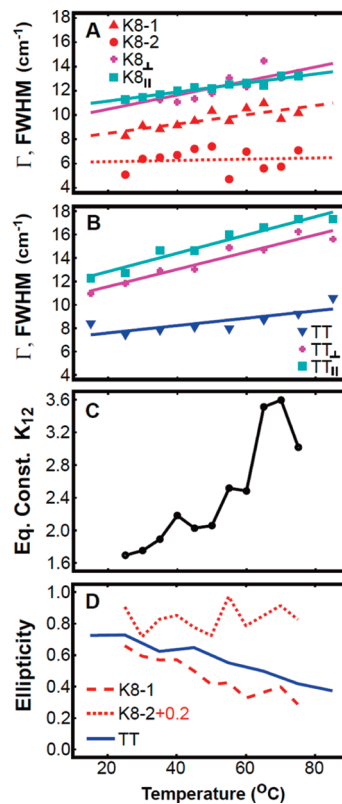


Figure 7. Lineshape analysis of temperature-dependent 2D IR spectra of K8 and TT. Antidiagonal line width (FWHM) for (A) K8 and (B) TT. (C) Ratio of K8-2 to K8-1 peak volumes. (D) Ellipticity of isotope-shifted peaks. The data for K8-2 has been upshifted by 0.2 for clarity.

elongated peak to a symmetrically distributed peak as the temperature is raised. From 15 to 75°C , the antidiagonal ν_{TT} FWHM increases more than 2.0 cm^{-1} , and the ν_{TT} diagonal width decreases by a similar amount over the equivalent temperature range. These line width shifts show that the region around T3 and T10 are relatively rigid at low temperature but experience increased configurational fluctuations of the peptide groups and surroundings as the temperature is raised. Yet, on average the frequency of the ν_{TT} peak and magnitude of cross-strand coupling remains unchanged from lower temperatures. These disordering pathways are consistent with the fraying transition described in previous hairpin simulations.^{30,84,85}

Simulation Results. To better interpret how the observed amide I spectral features report on peptide conformation, structure-based modeling of 2D IR spectra was applied to five sets of TZ2 conformers drawn from the Markov state analysis of Chodera et al.²⁹ Each configuration chosen for the spectral simulations should be viewed as an ansatz from which structural features can be identified that play an important role in determining the spectroscopy. One representative structure from each Markov state chosen is shown at the top of Figure 8, but conformational disorder varies for each of these states, as shown in the Supporting Information. Specifically, we focused on the following five conformational ensembles:

- “Folded” (FO, 250851) is a well-ordered ensemble that has an average of four backbone hydrogen bonds, which correspond to those in the NMR structure.²¹ The S1, T3, K8, and T10 carbonyls are all oriented for cross strand hydrogen bonds, and all four tryptophan side chains are packed to one face of the peptide.

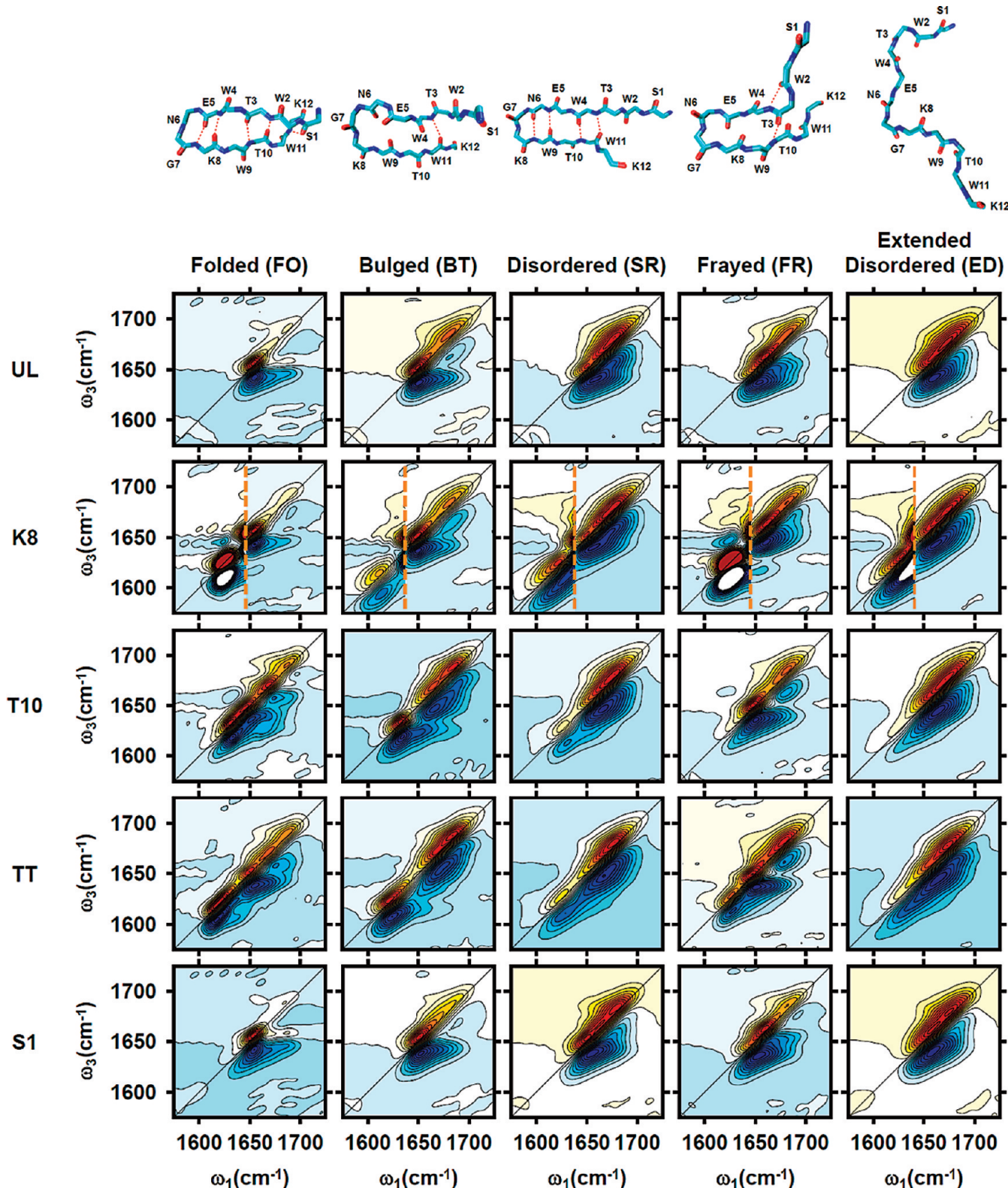


Figure 8. 2D IR spectral simulations of all five TZ2 isotopologues studied for five different conformational ensembles. One representative structure for each conformer macrostate is presented. Simulations of K8 for the spectral region $\omega_1 < 1650$ cm⁻¹ have the amplitudes scaled by a factor of 10×.

•“Bulged Turn” (BT, 214369) is a compact coiled structure with a well-solvated, bulged turn region and an average of one cross-strand hydrogen bond that appears near the strand termini. This state contains S1, T3, K8, and T10 peptide carbonyls that are solvent exposed, and tryptophan side chains make rare contacts.

•“Disordered” (SR, 271154) is a disordered ensemble whose common feature is a bulged turn and an average of one backbone hydrogen bond with a misaligned registry near the C terminus. Tryptophans are poorly organized.

•“Frayed” (FR, 11131) has a compact properly formed type I' turn region with an average of two backbone hydrogen bonds,

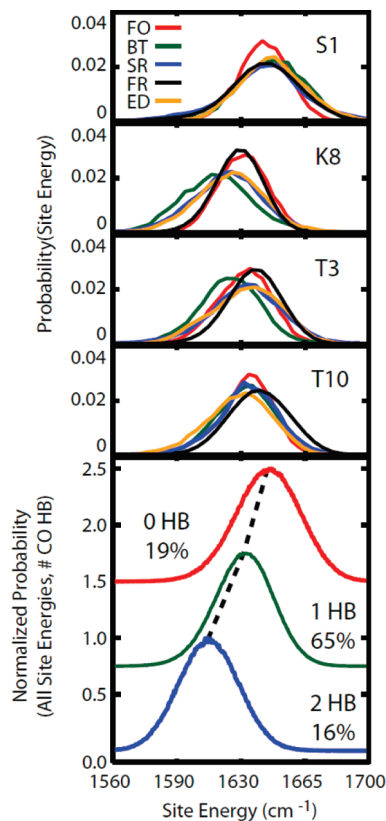


Figure 9. (Top) Isotope-labeled TZ2 amide I site energy distributions for the five Markov states. (Bottom) Distribution of calculated amide I site energies grouped by number of hydrogen bonds. A linear fit to the mean value gives $\omega = 1645.7 \text{ cm}^{-1} - 16.3 \times (\text{no. of CO H-bonds})$.

but disordered strand termini. The T3 and T10 are oriented toward the opposite strand, and tryptophan side chains are disordered.

•“Extended Disorder” (ED, 64336) is an extended and well-solvated state with substantial disorder and rare backbone hydrogen bonds.

Here the number identifying each state refers to the designation in Supporting Information for ref 28.

As a first point of contact to experiment, we used electric field mapping to calculate histograms of amide I site energies for the 11 peptide units of the backbone. The red-shift is primarily sensitive to hydrogen bonding to the oxygen site. Histograms for sites S1, T3, K8, and T10 are shown in Figure 9, with the remainder in the Supporting Information. It is apparent that the distribution of site energies for site T3 and K8 vary in such a way that the mean frequency is unique for the FO and BT conformers. On the other hand, S1 and T10 appear to be insensitive to conformation. Time-correlation functions for the site energy showed biphasic behavior, with a picosecond component attributed to solvent induced dephasing, and a longer component assigned to sampling of backbone configurations. The longer decay time varied from ~50 ps for S1, T3, and T10 to >200 ps for W4 and K8.

Our modeling of all conformers provides a general relationship between the amide I site frequency and the hydrogen bonds it participates in. We find that a hydrogen bond (HB) of an amide carbonyl to protein gives about the same red shift as a hydrogen bond to water. (For our purposes, in simulations a HB is defined by the hydrogen bond distance and angle: $r_{X \cdots O} \leq 4.5 \text{ \AA}$, $\theta_{X \cdots HO} < 35^\circ$.) However, when an amide group is

fully solvated by water, it has the ability to form multiple HBs, giving a larger average red shift. From analysis of both types of HBs, we find that on average, one HB leads to an 11 cm^{-1} red shift, however the dispersion in this relationship ($\sigma = 25 \text{ cm}^{-1}$) leads only to a modest correlation ($\rho = -0.50$). These results can be compared with the results of ab initio calculations on isolated clusters, which reveal a 20 cm^{-1} red-shift for each HB to oxygen and an additional 10 cm^{-1} red shift for hydrogen bonds donated by the peptide N–H.⁸⁶

For each of these five conformers, we simulated the infrared spectroscopy of the five isotopologues studied here. Simulated FTIR and FTIR difference spectra for each structure are shown in the Supporting Information section. In general we find that qualitative similarities exist between several of the experimental and simulated spectra, which we discuss in terms of peak positions, amplitudes, linewidths, and lineshapes. The simulated 2D IR spectra of the unlabeled peptide for FO, BT, and FR conformers each display two diagonal peaks and Z-shaped contours that resemble the experiment at low temperatures. For the disordered SR state, two bands are also resolved although in this case, the high-frequency band carries most of the intensity. Limiting the simulation only to a specific structure with +1C slipped registry and 4 hydrogen bonds leads to a spectrum similar to BT (see the Supporting Information). For the disordered ED state, the amide I band has little structure and reflects the diagonally stretched resonance of an inhomogeneous line shape.

As expected, each of the five K8 simulations gives rise to one resonance for the labeled site, although the peak position and line width vary with conformation. In particular, we see a correlation between the orientation and solvent exposure of the K8 amide group and the frequency of the isotope-shifted peak. In the case of FO and FR states each have a K8 amide group oriented so that its carbonyl oxygen forms a cross-strand hydrogen bond with the W4 amide proton, as expected for a type I' β turn. In their calculated spectra, the ν_{K8} peak is split from the amide I maximum by $25\text{--}30 \text{ cm}^{-1}$, and the diagonal line width is a compact $5\text{--}6 \text{ cm}^{-1}$. In addition, a distinct cross peak is observed between the ν_{K8} and ν_{\perp} bands in the calculated spectra for these states. For each of the other structures (SR, BT, and ED) the K8 oxygen has higher water exposure on average, although with higher variance in hydrogen bonds formed. The $\nu_{K8}\text{--}\nu_{\perp}$ amide I peak splitting for each of the corresponding spectra is $30\text{--}36 \text{ cm}^{-1}$, and the label resonance has distinctly broader diagonal linewidths of $10\text{--}14 \text{ cm}^{-1}$. The calculated BT spectrum shows the largest shift and line width. The observed differences can be attributed to variation in hydrogen bonding to the K8 carbonyl. Fully solvated carbonyls will on average participate in two hydrogen bonds to water, as opposed to one cross-strand hydrogen bond in the case of properly folded β turns. For the K8 carbonyl, we find that each hydrogen bond contributes on average a 16 cm^{-1} red shift in amide I frequency; however, the correlation between hydrogen bond number and red-shift is mild ($\rho = -0.53$). Therefore the solvent-exposed K8 conformers should exhibit an additional red shift relative to FO, but the conformational disorder and fluctuations in peptide backbone and water hydrogen bonds will also lead to a larger inhomogeneous width. Based on these observations, we conclude that the ν_{K8-1} peak represents peptides with non-native turns, and the high frequency ν_{K8-2} peak reports on structures with native type I' β -turns.

During simulations of the IR spectra for the NMR structure at pH 2.5, a correlation between the K8 site frequency and two distinct E5 side chain configurations was observed. Specifically,

two configurations of the glutamic acid side chain and backbone dihedrals that differed in O(K8)…>δC(E5) separation by 6.1 and 6.8 Å were predicted to be observed with frequency splitting of 12 cm⁻¹. The observation of these two conformers required a protonated form of the glutamic acid (pK_a 4.6). We ruled this out as an explanation of the two K8 peaks in experiments because the amide I resonances in FTIR and 2D IR spectra exhibit no pH dependence between pH 2.5 and 7.

The T10 peptide carbonyl adopts a variety of conformations in the Markov states simulated. In the case of the FO and FR states it is oriented for a cross-strand hydrogen bond, for BT it is entirely solvent exposed, and for SR and ED it samples a variety of configurations. In simulated spectra we note that a conformer with solvent exposed T10 carbonyl gives rise to a structured excitonic spectrum and a red-shifted and spectrally distinct T10 peak, whereas the internally hydrogen bonded site gives a peak merged with the excitonic band, as observed in experiment. For the SR and ED states, the intensity of the labeled transition is greatly diminished over the intense band seen in the completely water-exposed state. Of all simulations, the FR state corresponds best to the low temperature experimental spectra. These observations demonstrate that the T10 experimental spectra provide evidence of a T10 carbonyl that participates in a single cross-strand hydrogen bond over the temperature range sampled.

For 2D simulations of TT, we find that all conformers except ED have a resolvable red-shifted peak arising from the TT label. In the case of the disordered states SR and ED, there is little change in the spectrum between the T10 and TT simulations, which reflects the limited correlation between the positions of their T3 and T10 peptide units. For the FO and FR conformers, which have close T3-T10 contacts, a distinct ν_{TT} peak is observed although the T10 spectrum showed no distinct T10 isotope-shifted feature. This is a result of the additional red-shift of the ν_{TT} band as a result of T3-T10 amide I' coupling, which varies between 6–7 cm⁻¹ for the FO conformers and leads to a ν_{TT} – ν_⊥ splitting of >30 cm⁻¹. Comparing the T10 and TT 2D spectra for the BT state shows few differences besides additional inhomogeneous broadening of the ν_{TT} transition. Each of the simulated spectra containing proximal T3 and T10 sites bear similarity to the experimental spectra, but those that compare favorably to the calculated T10 and TT spectra are FR and FO. Finally, we note that the intensity of the simulated ν_{TT} feature scales with the strength of coupling between the two threonine sites. From these observations, we conclude that contacts between strands in the central region of the peptide exist throughout the temperature range studied. We also conclude that out-of-registry structure is not significantly populated in the equilibrium conditions observed here.

Simulations of the S1 spectrum were used to address the lack of a distinct peak for the ¹⁸O peptide site, and the shifts in intensity and line shape seen in FTIR and 2D IR spectra. In general, for the Markov states studied, the S1 site is protected from the solvent, because the serine side chain and terminal -NH₃⁺ both prefer to be oriented to the solvent, and because tryptophan side chains interfere with water penetration to the S1 carbonyl. Thus, the S1 site energies are generally high regardless of conformation. The FO state has many intact S1–W11 hydrogen bonds, the SR has S1 carbonyls that experience a range of solvent and side chain environments, and the FR is the most solvent exposed.

The experimental (S1-UL) FTIR difference spectrum indicates that intensity is lost at 1675 and 1640 cm⁻¹ upon S1 labeling. Simulations of this spectrum for various conformers shows that

this characteristic double peak loss feature matches those observed in the FO state, whereas other states show a single loss feature (see Supporting Information). Cross-strand hydrogen bonding between the S1 and W11 in the FO state lead to strong coupling across the β-strand and a low frequency ν_⊥-like mode which is decoupled from the rest of the band and shifts upon ¹⁸O isotope-labeling. However, the high frequency loss features in FTIR and 2D IR are also present in BT, SR, and FR, which have high site energies and weak coupling to the remaining peptide units. ¹⁸O labeling shifts the S1 vibrational frequency for each system from very high energies (≥1700 cm⁻¹) in the unlabeled spectrum to frequencies just to the blue of the ν_⊥. The distribution of S1 configurations available in these conformers suggests that the S1 site is generally disordered at all temperatures.

Discussion and Conclusions

Spectral changes to the amide I band of TZ2, using four isotopic substitutions to probe the β-turn (K8), the N-terminus (S1), and the midstrand region (T10 and TT) of the hairpin structure, provide a site-specific description of the thermal denaturation of this β hairpin. The ¹³C' label at K8 reveals two unique turn geometries, the type I' β-turn observed in the NMR structure (ν_{K8-2}), and a less populated disordered or bulged loop (ν_{K8-1}). Structural disorder within the ν_{K8-2} band does not increase significantly with temperature, from which we conclude that the β-turn structures remain well-ordered. The ν_{K8-1} population in contrast does decay with temperature, indicating a relatively unstable loop. The hairpin retains interstrand contacts in the midstrand T3-T10 region over the entire temperature range studied as evidenced by the consistently high frequency of the T10 resonance and coupling-shifted TT resonance. Unlike ν_{K8-2}, the 2D ν_{TT} line shape changes from a heterogeneously broadened peak to a more symmetric homogeneously broadened peak, indicating that this region experiences an increase in the magnitude of picosecond fluctuations in the peptide, its internal contacts, and immediate surroundings. Spectroscopy of the N-terminal serine group amide group puts constraints on the possible conformations of the termini. From our observations, we believe that S1 is free to explore a large configurational space, relative to the other labeled residues. These vary from structures in which the S1 amides are hydrogen bonded to the W11 amide to structures in which there is no interaction with the other peptide amides.

Additional information on the TZ2 turn is available from recent experiments on turn labeled TZ2-G7* and spectroscopic simulations based on the NMR structure.^{17,87} An isotope-shifted peak was well-resolved in the room temperature 2D IR spectrum, and shown to be consistent with a solvent exposed amide groups. In addition, 1 ps waiting-time 2D IR data revealed cross peak structure to the G7* site that was attributed to different solute–solvent substates. These observations are consistent with our assignments, and can be explained with our conformer simulations. The dominant isotope-shifted peak is at 1595 cm⁻¹, reflecting the high degree of solvent exposure of the G7 carbonyl observed in the FO structure. Other conformers studied have lower solvent exposure and considerable disorder, leading to higher transition frequencies, as observed in experiment.

The picture that emerges from these data provides a detailed view of a heterogeneous thermal fraying process. The 25 °C state includes roughly 60% conformers that retain most of the cross-strand contacts seen in the NMR structure, whereas others have midstrand hydrogen bonding contacts and a bulged loop. As temperature is raised, the ends fray for all molecules,

becoming more solvent exposed, and introducing more disorder into the central contacts of the hairpin. Contacts remain within the central region of the hairpin, but on average the turn is more ordered. No idealized unfolded state with fully solvated backbone is observed. These results add structural insight to the building body of evidence that TZ2 folding is heterogeneous.^{30,38,88} Further, these data provide a point of reference for testing the conformational variation and energy landscape observed by TZ2 molecular dynamics simulations.^{26,29,30,39,46}

These results also provide insight into the kinetics observed in temperature-jump unfolding experiments.¹⁶ We have evidence of different compact conformers and that the extended state is never realized under the conditions studied here. Therefore T-jump experiments do not characterize an idealized transition from folded to random coil structure. Instead such experiments characterize the shifting distribution of conformational substates, and changes in thermal disorder within those minima. In the future, transient T-jump 2D IR experiments will provide an avenue to more directly follow the evolution of conformational distributions.^{16,89} Such experiments could use folding rates to test for a correspondence of our K8 conformers with the Trp fluorescence wavelength dependent folding rates observed by Gruebele.³⁸

Curiously, the type I' turn appears to be favorable at high temperature. One can rationalize the origin of this apparent annealing by comparison of Markov states. The frayed state provides the possibility of packing W4 and W9 side chains about the turn which is not possible with the bulged turn. As such it appears that the desolvation entropy for water about tryptophans plays a key role in determining the relative stability of these conformers. This counterintuitive shift of turn stability could be compared with cold-denaturing transitions attributed to hydrophobic hydration.⁹⁰

What can we say about the TZ2 and the folding pathways of β hairpins? While it was originally assumed that there is a choice to be made between zipping⁴⁰ and hydrophobic collapse,⁹¹ it appears that both of these processes play crucial roles for the folding of TZ2. For TZ2, the simulations seem to be in agreement that folding proceeds from the turn to the termini, but that this “zip-out” process involves both contacts between W4 and W9 and turn hydrogen bonding contacts.^{28,39,92} This hybrid zipper type model^{45,93} explains the varying experimental views that both the nature of the turn and the hydrophobic packing²³ are critical to hairpin folding.

Our observations closely match those of Gao and co-workers,^{22,94} who recently performed MD simulations of the sequence dependent temperature-dependence of β hairpin folding. Temperature-dependent studies of TZ2 unfolding indicated that there was a propensity for the HB closest to the turn (E5-G7) to form as the temperature is raised, even though other HB tended to rupture. These authors used clustering analysis of states during TZ2 folding to argue that the folding mechanism from an extended state is dominated by a zip-out mechanism in which the turn forms first, although they do identify bulged configurations along the folding path.^{22,94} Hydrophobic clustering and cross-strand HBs were favorable at low temperature in the central region, whereas the frayed state was favored at high temperature.

Recently there have been several studies of peptide structure with isotope-labeled 2D IR spectroscopy that demonstrate the capabilities of this method for insight into backbone conformation and hydrogen bonding environment.^{11,19,20,51} This work indicates the potential of the method to unravel systems with conformational heterogeneity and disorder. With an appropriately large set of trial conformers and increased improvements in spectroscopic modeling, one should be able to use self-consistent modeling of multiple

isotopologues to provide a detailed picture of the global range of conformations adopted by the peptide. Experimentally, one can also imagine that for cases such as TZ2, 3D IR spectroscopy on multiply labeled peptides can provide a higher level of conformational detail by correlating the local structural environment between multiple sites of the same peptide. Such experiments provide an avenue to characterize conformational heterogeneity of rapidly exchanging conformers of proteins and peptides in folded and disordered states.

Acknowledgment. We thank Bill Swope for providing us with the Markov states²⁹ used in our modeling. We are indebted to John Chodera, Vijay Pande, Jed Pitner, and Bill Swope for extensive conversations on the simulation and analysis of TZ2 folding mechanisms and heterogeneity. For advice on various steps in the peptide synthesis, we thank Khaled A. Nasr and Dan Kemp. Additional technical support was provided by Jongjin Kim. This work was supported by the U.S. National Science Foundation (CHE-0316736, CHE-0616575, and CHE-0911107 to A.T.), the U.S. Department of Energy (DE-FG02-99ER14988 to A.T.), the David and Lucile Packard Foundation, and the ACS Petroleum Research Fund. Z.G. thanks the Poitras Predoctoral Fellowship for Fellowship support. T.L.C.J. acknowledges The Netherlands Organization for Scientific Research (NWO) for support through a VIDI grant.

Supporting Information Available: Details on the synthesis and calculations including (1) mass spectra of the synthesized peptides, (2) temperature dependent trends in FTIR and 2DIR spectra of TZ2 isotopologues, (3) table of spectral features in simulated 2D IR spectra of TZ2 isotopologues, (4) visualization of Markov states, (5) histograms of TZ2 site energies from simulations, (6) analysis of site frequency shifts as a function of hydrogen bonding, and (7) spectral simulations for single structures. This material is available free of charge via the Internet at <http://pubs.acs.org>.

References and Notes

- (1) Dyson, H. J.; Wright, P. E. *Chem. Rev.* **2004**, *104*, 3607.
- (2) Mourad, S.; Fushman, D.; Munoz, V. *Nature* **2006**, *442*, 317.
- (3) Tang, C.; Iwahara, J.; Clore, G. M. *Nature* **2006**, *444*, 383.
- (4) Iwahara, J.; Clore, G. M. *Nature* **2006**, *440*, 1227.
- (5) Mittermaier, A.; Lewis, E. K. *Science* **2006**, *312*, 224.
- (6) Palmer, A. G., III. *Curr. Opin. Struct. Biol.* **1997**, *7*, 732.
- (7) Akke, M.; Liu, J.; Cavanagh, J.; Erickson, H. P.; Palmer, A. G., III. *Nat. Struct. Biol.* **1998**, *5*, 55.
- (8) Palmer, A. G., III. *Annu. Rev. Biophys. Biomol. Struct.* **2001**, *30*, 129.
- (9) Ganim, Z.; Chung, H. S.; Smith, A. W.; Deflores, L. P.; Jones, K. C. *Acc. Chem. Res.* **2008**, *41*, 432.
- (10) Kim, Y. S.; Hochstrasser, R. M. *J. Phys. Chem. B* **2009**, *113*, 8231.
- (11) Mukherjee, P.; Kass, I.; Arkin, I. T.; Zanni, M. T. *Proc. Natl. Acad. Sci. U.S.A.* **2006**, *103*, 3528.
- (12) Sengupta, N.; Maekawa, H.; Zhuang, W.; Toniolo, C.; Mukamel, S.; Tobias, D. J.; Ge, N.-H. *J. Phys. Chem. B* **2009**, *113*, 12037.
- (13) Zhuang, W.; Hayashi, T.; Mukamel, S. *Angew. Chem., Int. Ed.* **2009**, *48*, 3750.
- (14) Jeon, J.; Yang, S.; Choi, J.-H.; Cho, M. *Acc. Chem. Res.* **2009**, *42*, 1280.
- (15) Khalil, M.; Demirdoven, N.; Tokmakoff, A. *J. Phys. Chem. A* **2003**, *107*, 5258.
- (16) Chung, H. S.; Ganim, Z.; Jones, K. C.; Tokmakoff, A. *Proc. Natl. Acad. Sci. U.S.A.* **2007**, *104*, 14237.
- (17) Wang, J.; Zhuang, W.; Mukamel, S.; Hochstrasser, R. *J. Phys. Chem. B* **2008**, *112*, 5930.
- (18) Kim, Y. S.; Liu, L.; Axelsen, P. H.; Hochstrasser, R. M. *Proc. Natl. Acad. Sci. U.S.A.* **2008**, *105*, 7720.
- (19) Maekawa, H.; De Poli, M.; Toniolo, C.; Ge, N.-H. *J. Am. Chem. Soc.* **2009**, *131*, 2042.
- (20) Shim, S.-H.; Gupta, R.; Ling, Y. L.; Strasfeld, D. B.; Raleigh, D. P.; Zanni, M. T. *Proc. Natl. Acad. Sci. U.S.A.* **2009**, *106*, 6614.

- (21) Cochran, A. G.; Skelton, N. J.; Starovasnik, M. A. *Proc. Natl. Acad. Sci. U.S.A.* **2001**, *98*, 5578.
- (22) Yang, L.; Shao, Q.; Gao, Y. Q. *J. Phys. Chem. B* **2009**, *113*, 803.
- (23) Wu, L.; McElheny, D.; Huang, R.; Keiderling, T. A. *Biochemistry* **2009**, *48*, 10362.
- (24) Smith, A. W.; Chung, H. S.; Ganim, Z.; Tokmakoff, A. *J. Phys. Chem. B* **2005**, *109*, 17025.
- (25) Hauser, K.; Krejtschi, C.; Huang, R.; Wu, L.; Keiderling, T. A. *J. Am. Chem. Soc.* **2008**, *130*, 2984.
- (26) Singhal, N.; Snow, C.; Pande, V. S. *J. Chem. Phys.* **2004**, *121*, 415.
- (27) Jansen, T. L. C.; Knoester, J. *Biophys. J.* **2008**, *94*, 1818.
- (28) Xiao, Y.; Chen, C.; He, Y. *Int. J. Mol. Sci.* **2009**, *10*, 2838.
- (29) Chodera, J. D.; Singh, N.; Pande, V. S.; Dill, K. A.; Swope, W. C. *J. Chem. Phys.* **2007**, *126*, 155101.
- (30) Yuan Yang, W.; Pitera, J. W.; Swope, W. C.; Gruebele, M. *J. Mol. Bio.* **2004**, *336*, 241.
- (31) Kubelka, J.; Hofrichter, J.; Eaton, W. A. *Curr. Opin. Struct. Biol.* **2004**, *14*, 76.
- (32) Searle, M. S.; Ciani, B. *Current Opinion in Structural Biology* **2004**, *14*, 458.
- (33) Karplus, M.; Weaver, D. L. *Protein Sci.* **1994**, *3*, 650.
- (34) Kim, P. S.; Baldwin, R. L. *Annu. Rev. Biochem.* **1982**, *51*, 459.
- (35) Ptitsyn, O. B. *J. Protein Chem.* **1987**, *6*, 273.
- (36) Christopher, M.; Dobson, A. S.; Karplus, M. *Angew. Chem., Int. Ed.* **1998**, *37*, 868.
- (37) Ptitsyn, O. B. *Adv. Protein Chem.* **1995**, *47*, 83.
- (38) Yang, W. Y.; Gruebele, M. *J. Am. Chem. Soc.* **2004**, *126*, 7758.
- (39) Snow, C. D.; Qiu, L.; Du, D.; Gai, F.; Hagen, S. J.; Pande, V. S. *Proc. Natl. Acad. Sci. U.S.A.* **2004**, *101*, 4077.
- (40) Muñoz, V.; Thompson, P. A.; Hofrichter, J.; Eaton, W. A. *Nature* **1997**, *390*, 196.
- (41) Du, D.; Zhu, Y.; Huang, C.-Y.; Gai, F. *Proc. Natl. Acad. Sci. U.S.A.* **2004**, *101*, 15915.
- (42) Du, D.; Matthew J., T.; Gai, F. *Biochemistry* **2006**, *45*, 2668.
- (43) Brian, D. R.; Maness, S. J.; Peterson, E. S.; Franzen, S.; Fesinmeyer, R. M.; Andersen, N. H. *Biochemistry* **2004**, *43*, 11560.
- (44) Olsen, K. A.; Fesinmeyer, R. M.; Stewart, J. M.; Andersen, N. H. *Proc. Natl. Acad. Sci. U.S.A.* **2005**, *102*, 15483.
- (45) Tsai, J.; Levitt, M. *Biophys. Chem.* **2002**, *101*–*102*, 187.
- (46) Pitera, J. W.; Haque, I.; Swope, W. C. *J. Chem. Phys.* **2006**, *124*, 141102.
- (47) Fang, C.; Wang, J.; Charnley, A. K.; Barber-Armstrong, W.; Smith, A. B., III; Decatur, S. M.; Hochstrasser, R. M. *Chem. Phys. Lett.* **2003**, *382*, 586.
- (48) Fang, C.; Hochstrasser, R. M. *J. Phys. Chem. B* **2005**, *109*, 18652.
- (49) Kim, Y. S.; Liu, L.; Axelsen, P. H.; Hochstrasser, R. M. *Proc. Natl. Acad. Sci. U.S.A.* **2009**, *106*, 17751.
- (50) Manor, J.; Mukherjee, P.; Lin, Y.-S.; Leonov, H.; Skinner, J. L.; Zanni, M. T.; Arkin, I. T. *Structure* **2009**, *17*, 247.
- (51) Maekawa, H.; De Poli, M.; Moretto, A.; Toniolo, C.; Ge, N.-H. *J. Phys. Chem. B* **2009**, *113*, 11775.
- (52) Kim, Y. S.; Liu, L.; Axelsen, P. H.; Hochstrasser, R. M. *Proc. Natl. Acad. Sci. U.S.A.* **2008**, *105*, 7720.
- (53) Demirdoven, N.; Cheatum, C. M.; Chung, H. S.; Khalil, M.; Knoester, J.; Tokmakoff, A. *J. Am. Chem. Soc.* **2004**, *126*, 7981.
- (54) Ganim, Z.; Tokmakoff, A. *Biophys. J.* **2006**, *91*, 2636.
- (55) Hayashi, T.; Zhuang, W.; Mukamel, S. *J. Phys. Chem. A* **2005**, *109*, 9747.
- (56) Choi, J.-H.; Ham, S.; Cho, M. *J. Phys. Chem. B* **2003**, *107*, 9132.
- (57) Jansen, T. L. C.; Dijkstra, A. G.; Watson, T. M.; Hirst, J. D.; Knoester, J. *J. Chem. Phys.* **2006**, *125*, 044312.
- (58) Jansen, T. L. C.; Knoester, J. *J. Chem. Phys.* **2006**, *124*, 044502.
- (59) Schmidt, J. R.; Corcelli, S. A.; Skinner, J. L. *J. Chem. Phys.* **2004**, *121*, 8887.
- (60) Lin, Y.-S.; Shorb, J. M.; Mukherjee, P.; Zanni, M. T.; Skinner, J. L. *J. Phys. Chem. B* **2009**, *113*, 592.
- (61) Roberts, S. T.; Loparo, J. J.; Tokmakoff, A. *J. Chem. Phys.* **2006**, *125*.
- (62) Smith, A. W.; Tokmakoff, A. *J. Chem. Phys.* **2007**, *126*, 045109.
- (63) Mawhinney, T. P.; Madson, M. A. *J. Org. Chem.* **1982**, *47*, 3336.
- (64) Lindahl, E.; Hess, B.; van der Spoel, D. *J. Mol. Mod.* **2001**, *7*, 306–317. *J. Mol. Model.* **2001**, *7*, 306.
- (65) Berendsen, H. J. C.; van der Spoel, D.; van Drunen, R. *Comput. Phys. Commun.* **1995**, *91*, 43.
- (66) Jorgensen, W. L.; Maxwell, D. S.; Tirado-Rives, J. *J. Am. Chem. Soc.* **1996**, *118*, 11225.
- (67) Jorgensen, W. L.; McDonald, N. A. *J. Mol. Struct.* **1998**, *424*, 145.
- (68) McDonald, N. A.; Jorgensen, W. L. *J. Phys. Chem. B* **1998**, *102*, 8049.
- (69) Rizzo, R. C.; Jorgensen, W. L. *J. Am. Chem. Soc.* **1999**, *121*, 4827.
- (70) Price, M. L.; Strovsky, D. O.; Jorgensen, W. L. *J. Comput. Chem.* **2001**, *22*, 1340.
- (71) Watkins, E. K.; Jorgensen, W. L. *J. Phys. Chem. A* **2001**, *105*, 4118.
- (72) Kaminski, G. A.; Tirado-Rives, J.; Friesner, R. A.; Jorgensen, W. L. *J. Phys. Chem. B* **2001**, *105*, 6474.
- (73) Essman, U.; Perela, L.; Berkowitz, M. L.; Darden, T.; Lee, H.; Pedersen, L. G. *J. Chem. Phys.* **1995**, *103*, 8577.
- (74) Berendsen, H. J. C.; Grigera, J. R.; Straatsma, T. P. *J. Phys. Chem.* **1987**, *91*, 6269.
- (75) Berendsen, H. J. C.; Postma, J. P. M.; van Gunsteren, W. F.; DiNola, A.; Haak, J. R. *J. Chem. Phys.* **1984**, *81*, 3684.
- (76) Miyamoto, S.; Kollman, P. A. *J. Comput. Chem.* **1992**, *13*, 952.
- (77) Eisenberg, D.; McLachlan, A. D. *Nature* **1986**, *319*, 199.
- (78) Hess, B.; Bekker, H.; Berendsen, H. J. C.; Fraaije, J. G. E. M. *J. Comput. Chem.* **1997**, *18*, 1463.
- (79) Jansen, T. L. C.; Knoester, J. *Acc. Chem. Res.* **2009**, *42*, 1405.
- (80) Jansen, T. L. C.; Knoester, J. *J. Phys. Chem. B* **2006**, *110*, 22910.
- (81) Shraga, P.; Laulicht, I. *Infrared Spectra of Labelled Compounds*; Academic Press: New York, 1971.
- (82) Hauser, K.; Krejtschi, C.; Huang, R.; Wu, L.; Keiderling, T. A. *J. Am. Chem. Soc.* **2008**, *130*, 2984.
- (83) Lazonder, K.; Pshenichnikov, M. S.; Wiersma, D. A. *Opt. Lett.* **2006**, *31*, 3354.
- (84) Bolhuis, P. G. *Biophys. J.* **2005**, *88*, 50.
- (85) Bolhuis, P. G. *Proc. Natl. Acad. Sci. U.S.A.* **2003**, *100*, 12129.
- (86) Ham, S.; Kim, J.-H.; Lee, H.; Cho, M. *J. Chem. Phys.* **2003**, *118*, 3491.
- (87) Kim, Y. S.; Hochstrasser, R. M. *J. Phys. Chem. B* **2007**, *111*, 9697.
- (88) Huang, K. R.; Keiderling, T. A.; Hauser, K. *Vib. Spectrosc.* **2008**, *48*, 1.
- (89) Smith, A. W.; Tokmakoff, A. *Angew. Chem. Int. Ed.* **2007**, *46*, 7984.
- (90) Urry, D. W.; Hugel, T.; Seitz, M.; Gaub, H. E.; Sheiba, L.; Dea, J.; Xu, J.; Parker, T. *Phil. Trans. R. Soc. London B* **2002**, *357*, 169.
- (91) Dinner, A. R.; Lazaridis, T.; Karplus, M. *Proc. Natl. Acad. Sci. U.S.A.* **1999**, *96*, 9068.
- (92) Yang, W.; Nymeyer, H.; Zhou, H.-X.; Berg, B.; Schweiler, R. B. *J. Comput. Chem.* **2008**, *29*, 668.
- (93) Zhou, R.; Berne, B. J.; Germain, R. *Proc. Natl. Acad. Sci. U.S.A.* **2001**, *98*, 14931.
- (94) Shao, Q.; Wei, H. Y.; Gao, Y. Q. *J. Am. Chem. Soc.* 2009, submitted.

JP104017H